March 18, 2009

Size and geometry dependent protein-nanoparticle self-assembly

M De
OR Miranda
S Rana
VM Rotello

Size and geometry dependent protein–nanoparticle self-assembly†‡

Mrinmoy De, Oscar R. Miranda, Subinoy Rana and Vincent M. Rotello*

Received (in Austin, TX, USA) 12th January 2009, Accepted 18th February 2009
First published as an Advance Article on the web 18th March 2009
DOI: 10.1039/b900552h

Fundamentally different assembly motifs are observed when proteins of different sizes are complexed with monolayer-protected nanoparticles.

Protein–nanoparticle conjugates have numerous applications in biology and material science. Nanoparticle–protein interactions can control enzymatic behavior,[1] protein–protein interactions,[2] protein delivery[3] and be applied to sensors and diagnostics.[4] Assemblies of proteins with nanoparticles also provide building blocks for the creation of hybrid bionanomaterials.[5] The wide range of sizes and charges of protein molecules provide access to a broad range of biomaterials with controlled interparticle spacing,[6] magnetic properties[7] and overall structure of the nanocomposites. Each of these applications rely extensively on the fundamental aspects of protein–nanoparticle interactions. Monolayer-functionalized nanoparticles provide a tunable surface for binding with target molecules, enabling controlled nanoparticle–protein interactions. A fundamental understanding of the thermodynamic parameters of these protein–nanoparticle interactions provides an important foundation for the application of these systems in biological and material applications.

Isothermal titration calorimetry (ITC) provides a powerful tool for investigating the thermodynamics and stoichiometry of supramolecular processes.[8] ITC analysis can be used in nanoparticle–protein assemblies to determine: (i) binding stoichiometry, (ii) stability of the conjugates, and (iii) solubility or aggregation of the conjugates *etc*. Likewise, ITC analysis of protein–nanoparticle complexation can determine the nature of binding (entropic *vs*. enthalpic), and the effect of surface functionality and environmental conditions on binding ratios and affinities.[9]

In this communication, we report the thermodynamic characterization on the interaction of proteins of three different sizes with nanoparticles using ITC to probe the effect of relative particle–protein size in complexation (Fig. 1c). In these studies, we observe that when the particle is larger than the protein, multiple proteins bind to each particle. When the sizes are commensurate, extended aggregates are formed, and when the protein is larger than the particle multiple particles bind per protein.

For our studies we used 2 nm core gold nanoparticles (~8 nm overall diameter) with variable cationic functionality (hydrophobic, hydrophilic and aromatic, Fig. 1a). The selected proteins are anionic in nature to allow sufficient electrostatic interaction. For the protein, we choose three anionic proteins of distinctly different size (Fig. 1b). Green fluorescence protein (GFP) is the smallest beta barrel shaped protein among these: 3.0 nm × 4.0 nm (MW = 27 kDa, pI = 5.92).[10] Bovine serum albumin (BSA) is a triangular prismatic protein with comparable size to the nanoparticle: 8.4 nm × 8.4 nm × 8.4 nm × 3.1 nm (MW = 66.3 kDa, pI = 4.8).[11] The third protein is acid phosphatase (PhosA), which is orthorhombic shaped and larger than the receptors: 12.6 nm × 20.7 nm × 7.3 nm (MW = 110 kDa, pI = 5.2).[12]

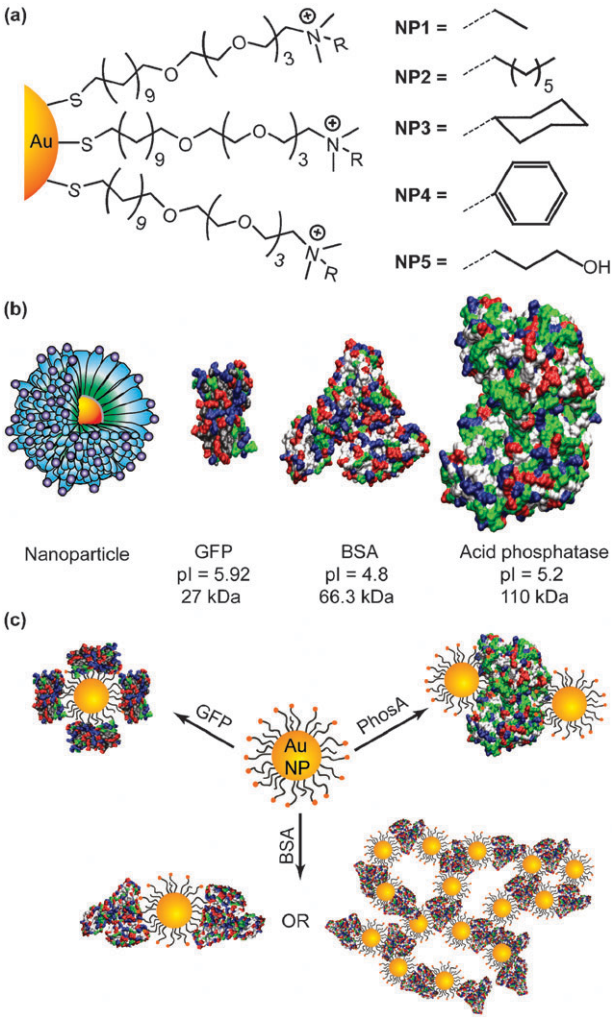

Fig. 1 (a) Chemical structure of the cationic gold nanoparticles (**NP1–NP5**). (b) Surface structural features and relative size of three negatively charged proteins used in the ITC study. Color scheme for the proteins: basic residues (blue), acidic residues (red), polar residues (green) and non-polar residues (gray). (c) Schematic depiction of particle–protein assemblies observed in this study.

Department of Chemistry, University of Massachusetts at Amherst, Amherst, MA 01003, USA. E-mail: rotello@chem.umass.edu
† Dedicated to Julius Rebek, a true pioneer in the field of supramolecular chemistry, on the occasion of his 65th birthday.
‡ Electronic supplementary information (ESI) available: Experimental details, ITC and DLS analysis. See DOI: 10.1039/b900552h

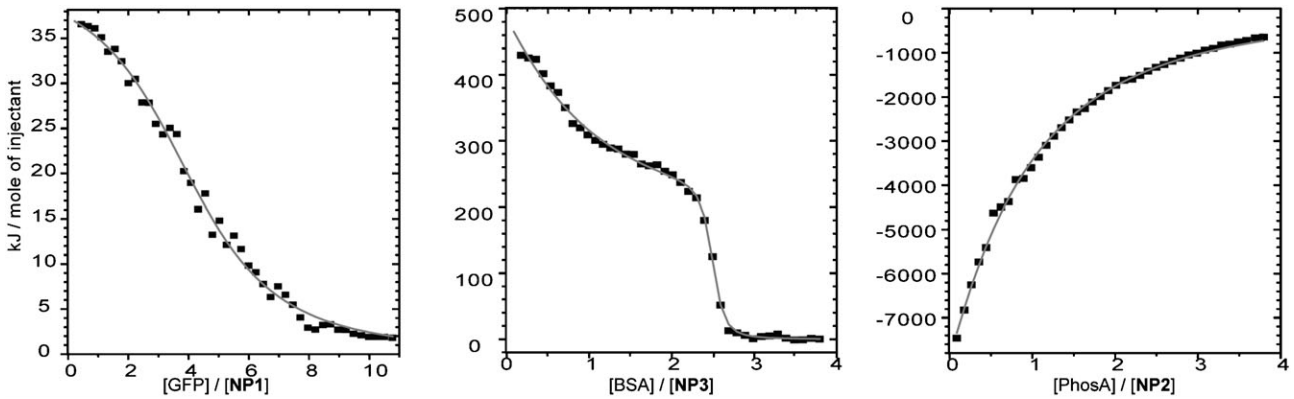

Fig. 2 ITC analysis for the complexation of (a) GFP with **NP1**, (b) BSA with **NP3**, and (c) PhosA with **NP2** in 5 mM sodium phosphate buffer (pH = 7.4). The squares represent the integrated heat changes during complex formation and the lines the curve fit to the binding isotherm.

The ITC experiments were carried out at 30 °C by titrating protein solutions into the nanoparticle solution. Depending on the protein structure we observed three different types of heat change profile from the titration curves (Fig. 2). The complexation of GFP[13] and BSA with all nanoparticles is endothermic in nature, while the complexation of PhosA with nanoparticles is exothermic. We fitted these enthalpies to determine the stoichiometries and affinities of the particle–protein dyads. The complexation of nanoparticles with GFP and PhosA can be fitted using a single set of identical nanoparticle binding sites. In contrast, the BSA with comparable size to the nanoparticles can only be assessed using a binding mode of two sets of binding sites. We also observed the precipitation at the end of titration, in contrast to the other two proteins. Using the isothermal curve fitting analysis various thermodynamic parameters such as binding constants (K_S), enthalpy changes (ΔH) and binding stoichiometries (n) were determined. The Gibbs free energy changes (ΔG) and entropy changes (ΔS) were calculated by using the standard thermodynamic equations: $\Delta G = -RT\ln K_S$ and $\Delta G = \Delta H - T\Delta S$. These quantities for the corresponding nanoparticle–protein interactions are summarized in Table 1.

Table 1 Complex stability constants (K_S), Gibbs free energy changes (ΔG), enthalpy changes (ΔH), entropy changes ($T\Delta S$), and binding stoichiometries (n) for the complexation of GFP, BSA and PhosA with various gold NPs (5 mM sodium phosphate, pH 7.4) at 30 °C

Protein	NPs	K_S/M^{-1}	$-\Delta G$/kJ mol^{-1}	ΔH/ kJ mol^{-1}	$T\Delta S$/ kJ mol^{-1}	n
GFP	**NP1**	1.74×10^6	36.22	42.26	78.48	4.39
BSA[a]	**NP1**	3.66×10^7	43.89	18.70	62.59	1.71
	NP2	9.63×10^7	46.33	223.43	269.76	1.89
	NP3	10.7×10^7	46.60	187.02	233.62	2.11
	NP4	26.5×10^7	48.88	247.27	296.15	2.27
	NP5	5.86×10^7	45.08	164.43	209.51	1.97
BSA[b,c]	**NP1**	1.21×10^8	46.91	1133.86	1180.77	0.36
	NP2	10.4×10^8	52.33	615.05	667.38	0.39
	NP3	3.13×10^8	49.30	1087.84	1137.14	0.34
	NP4	1.04×10^8	52.33	732.20	775.53	0.39
	NP5	8.46×10^8	51.81	623.42	675.23	0.32
PhosA	**NP1**	2.03×10^5	30.80	−11171	−11140	0.43
	NP2	1.47×10^5	29.99	−31380	−31350	0.45
	NP3	1.89×10^5	30.62	−29664	−29633	0.43
	NP4	1.69×10^5	30.34	−35103	−35073	0.39
	NP5	3.16×10^5	31.92	−21171	−21139	0.44

[a] First binding event. [b] Second binding event. [c] Binding parameters for nanoparticle–protein aggregation and precipitation.

An important observation from Table 1 is the binding ratios and binding mode between protein and nanoparticles which are drastically different depending on protein size. In the case of GFP the GFP–nanoparticle binding ratio is ~4 : 1. In contrast, for the larger protein PhosA the protein–nanoparticle binding ratio is ~1 : 2.5, indicating more nanoparticles are involved with single nanoparticle binding. In the case of BSA where size is commensurate there are two binding modes. In the first binding mode, the binding is similar to GFP, where each nanoparticle is surrounded by two BSA molecules. The second binding event involves nanoparticle–protein aggregation and precipitation. As we observed the aggregation at the end of the titration, the parameters obtained for the second binding event should be considered as apparent binding parameters. The apparent binding parameter is the combination of heat change during protein–nanoparticle assembly followed by aggregation. This extended aggregation and precipitation is supported by the large positive entropy change ($T\Delta S$ = 667–1180 kJ mol^{-1}) due to the release of numerous bound water molecules. This aggregation was further established by a dynamic light scattering (DLS) study (see ESI‡), where aggregates of ~150 nm were formed initially between **NP1** and BSA, with larger aggregates and concomitant precipitation observed over time. We did not observe any precipitation over long periods of time (24 h) at low ratios of BSA to nanoparticle. Hence, by keeping the ratio of BSA to nanoparticle <2 : 1, discrete complex formation is induced. However, increasing the ratio of BSA causes formation of a more extended assembly with concomitant precipitation. As we can see in Fig. 2b two discrete binding events are observed. While size is clearly an important determinant in the assembly process, it should be noted that other parameters such as charge distribution can also influence assembly.

The thermodynamic quantities listed in Table 1 indicate that the nanoparticle–protein interaction can be controlled by surface modification of artificial receptors. Further examination of the change of enthalpy and entropy values indicates that the complexation of GFP and BSA involves an unfavorable enthalpy change ($\Delta H > 0$) that is compensated by a favorable entropy gain ($\Delta S > 0$), resulting in an overall

negative free energy change (ΔG). On the other hand, the interaction with the larger protein, PhosA, is an exothermic process with highly negative change in enthalpy ($\Delta H < 0$), although this favorable gain is partially offset by unfavorable entropy loss ($\Delta S < 0$). These enthalpy or entropy controlled processes can be easily explained if we consider the overall complexation process as described in eqn (3), which is the combination of two simultaneous processes (eqn (1) and (2)).

$$\text{Protein} + \text{NP} \rightleftharpoons \text{Protein–NP} \quad (1)$$

$$x\text{H}_2\text{Op} + y\text{H}_2\text{On} \rightleftharpoons (x + y - z)\text{H}_2\text{Op–n} + z\text{H}_2\text{O} \quad (2)$$

$$\text{Protein}\cdot x\text{H}_2\text{Op} + \text{NP}\cdot y\text{H}_2\text{On} \rightleftharpoons \text{Protein–NP}\cdot(x + y - z)\text{H}_2\text{Op–n} + z\text{H}_2\text{O} \quad (3)$$

H_2Op, H_2On, H_2Op–n—water molecule associated with protein, nanoparticle and protein–nanoparticle complex, respectively.

The first process is a non-covalent complex formation, where ΔH and ΔS are both negative, *i.e.* an exothermic process. In contrast, the solvent reorganization process involves the disruption of well-defined solvent shells to generate an endothermic process ($\Delta H > 0$ and $\Delta S > 0$). Depending on the contribution of these two processes, the final complexation (eqn (3)) will be either exothermic (1st process predominant) or endothermic (2nd process predominant). In complexation of the smaller proteins, GFP and BSA, a higher degree of surface interaction is occurring that results from the release of a large amount of the water of hydration from the binding interface. This process is evident from the large positive entropy changes. On the other hand, protein–nanoparticle non-covalent interactions play the main role for the PhosA, as indicated by the observed negative enthalpy changes.

We also observed from Table 1 that enthalpy and entropy changes are always balanced to get a favorable free energy change ($\Delta G < 0$). This indicates that enthalpy–entropy compensation is operative, consistent with many host–guest processes.[14] The physical significance of enthalpy–entropy compensation is determined from the linear correlation using the relation $T\Delta S = \alpha\Delta H + T\Delta S_0$, where α is the slope and $T\Delta S_0$ is the intercept. The slope and intercept of the compensation plots have been related to the conformational change and desolvation during complexation, respectively.[15] As shown in Fig. 3, an excellent linear relationship is obtained for these thermodynamic quantities with a correlation coefficient of 0.999. Near-unit slopes ($\alpha = 1.00$) suggest that significant conformational changes occur at the interaction interface, which is similar to that found in other flexible systems such as protein–protein interactions ($\alpha = 1.00$ for protein–NP and 0.94 for protein–protein).[9a] For the nanoparticle systems, the reorganization of flexible surface ligands provides a target-responsive system to afford optimal binding affinity.[16] Large positive intercept values ($T\Delta S_0 = 46.2$ kJ mol^{-1}) are also obtained for these interactions, reflecting the extensive desolvation during complexation similar to protein–protein interactions ($T\Delta S_0 = 46.2$ kJ mol^{-1} for protein–NP and 41.5 kJ mol^{-1} for protein–protein).[9a]

In summary, we have demonstrated that the stoichiometry and thermodynamic properties for complexation between protein and nanoparticles depend on, among other considerations,

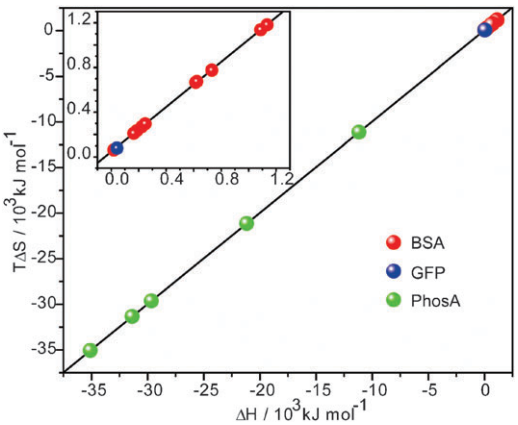

Fig. 3 Entropy ($T\Delta S$) *versus* enthalpy (ΔH) plot for protein–nanoparticle interaction. Inset shows magnification of the correlation data for BSA and GFP.

the relative size and surface functionality of the proteins. In these studies, we observed that with a protein smaller than the particle, one particle complexed multiple proteins, whereas when the protein was larger than the particle multiple particles complexed each protein. On the other hand extended self-assembly was observed for similar sized particle and protein.

The authors are grateful to the National Science Foundation (CHE-0808945).

Notes and references

1 C. C. You, M. De, G. Han and V. M. Rotello, *J. Am. Chem. Soc.*, 2005, **127**, 12873.
2 H. Bayraktar, P. S. Ghosh, V. M. Rotello and M. J. Knapp, *Chem. Commun.*, 2006, 1390.
3 W. Jiang, B. Y. S. Kim, J. T. Rutka and W. C. W. Chan, *Nat. Nanotechnol.*, 2008, **3**, 145.
4 (*a*) C. C. You, O. R. Miranda, B. Gider, P. S. Ghosh, I. B. Kim, B. Erdogan, S. A. Krovi, U. H. F. Bunz and V. M. Rotello, *Nat. Nanotechnol.*, 2007, **2**, 318; (*b*) R. L. Phillips, O. R. Miranda, C. C. You, V. M. Rotello and U. H. F. Bunz, *Angew. Chem., Int. Ed.*, 2008, **47**, 2590.
5 (*a*) R. A. McMillan, C. D. Paavola, J. Howard, S. L. Chan, N. J. Zaluzec and J. D. Trent, *Nat. Mater.*, 2002, **1**, 247; (*b*) M. H. Hu, L. P. Qian, R. P. Brinas, E. S. Lymar and J. F. Hainfeld, *Angew. Chem., Int. Ed.*, 2007, **46**, 5111.
6 (*a*) S. Srivastava, A. Verma, B. L. Frankamp and V. M. Rotello, *Adv. Mater.*, 2005, **17**, 617; (*b*) A. Verma, S. Srivastava and V. M. Rotello, *Chem. Mater.*, 2005, **17**, 6317.
7 S. Srivastava, B. Samanta, B. J. Jordan, R. Hong, Q. Xiao, M. T. Tuominen and V. M. Rotello, *J. Am. Chem. Soc.*, 2007, **129**, 11776.
8 I. Jelesarvo and H. I. Bosshard, *J. Mol. Recognit.*, 1999, **12**, 3.
9 (*a*) M. De, C. C. You, S. Srivastava and V. M. Rotello, *J. Am. Chem. Soc.*, 2007, **129**, 10747; (*b*) S. Lindman, I. Lynch, E. Thulin, H. Nilsson, K. A. Dawson and S. Linse, *Nano Lett.*, 2007, **7**, 914; (*c*) H. Joshi, P. S. Shirude, V. Bansal, K. N. Ganesh and M. Sastry, *J. Phys. Chem. B*, 2004, **108**, 11535.
10 R. Y. Tsien, *Annu. Rev. Biochem.*, 1998, **67**, 509.
11 M. L. Ferrer, R. Duchowicz, B. Carrasco, J. G. de la Torre and A. U. Acuna, *Biophys. J.*, 2001, **80**, 2422.
12 (*a*) M. Kruzel and B. Morawiecka, *Acta Biochim. Pol.*, 1982, **29**, 321; (*b*) C. G. Jakob, K. Lewinski, R. Kuciel, W. Ostrowski and L. Lebioda, *Prostate (N. Y., NY, U. S.)*, 2000, **42**, 211.
13 Complexation of GFP was studied with only one particle due to the large quantity of this bacterially-expressed protein required for titration.
14 K. N. Houk, A. G. Leach, S. P. Kim and X. Zhang, *Angew. Chem., Int. Ed.*, 2003, **42**, 4872.
15 M. V. Rekharsky and Y. Inoue, *Chem. Rev.*, 1998, **98**, 1919.
16 A. Boal and V. M. Rotello, *J. Am. Chem. Soc.*, 2000, **122**, 734.